Hydrogen bonding in different pyrimidine–methanol clusters probed by polarized Raman spectroscopy and DFT calculations

ARTICLE *in* JOURNAL OF RAMAN SPECTROSCOPY · APRIL 2011

Impact Factor: 2.67 · DOI: 10.1002/jrs.2744

8 AUTHORS, INCLUDING:

Dheeraj K Singh
Jacobs University Germany
28 PUBLICATIONS **178** CITATIONS
SEE PROFILE

Sunil Srivastava
Richmond Chemical Corporation
117 PUBLICATIONS **1,038** CITATIONS
SEE PROFILE

Juergen Popp
Friedrich Schiller University Jena
408 PUBLICATIONS **6,077** CITATIONS
SEE PROFILE

Ranjan K Singh
Banaras Hindu University
71 PUBLICATIONS **509** CITATIONS
SEE PROFILE

Research Article

Journal of RAMAN SPECTROSCOPY

Received: 7 October 2009 Accepted: 31 December 2009 Published online in Wiley Online Library: 2 August 2010

(wileyonlinelibrary.com) DOI 10.1002/jrs.2744

Hydrogen bonding in different pyrimidine–methanol clusters probed by polarized Raman spectroscopy and DFT calculations

Dheeraj K. Singh,[a] Shivangi Mishra,[a] Animesh K. Ojha,[b] Sunil K. Srivastava,[c] S. Schlücker,[c] B. P. Asthana,[a]* J. Popp[d] and Ranjan K. Singh[a]*

We report on the hydrogen bonding between pyrimidine (Pd) and methanol (M) as H-donor in this study. Hydrogen bonds between pyrimidine and methanol molecules as well as those between different methanol molecules significantly influence the spectral features at high dilution. The ring-breathing mode ν_1 of the reference system Pd was chosen as a marker band to probe the degree of hydrogen bonding. Polarized Raman spectra in the region 970–1020 cm^{-1} for binary mixtures of (pyrimidine + methanol) at 28 different mole fractions were recorded. A Raman line shape analysis of the isotropic Raman line profiles at all concentrations revealed three distinct spectral components at mole fractions of Pd below 0.75. The three components are attributed to three distinct groups of species: 'free Pd' (pd), 'Pd with low methanol content' (pd1) and 'Pd with high-methanol content' (pd2). The two latter species differ considerably in the pattern and the strengths of the hydrogen bonds. The results of density functional theory calculations on structures and vibrational spectra of neat Pd and eight Pd/M complexes with varying methanol content support our interpretations of the experimental results. A nice spectra–structure correlation for the different cluster subgroups was obtained, similar to earlier results obtained for Pd and water. Apart from N···H and O···H hydrogen bonds between pyrimidine and methanol, O···H hydrogen bonds formed among the methanol molecules in the cluster at high methanol content also play a crucial role in the interpretation of the experimental results.

Keywords: hydrogen bonding; pyrimidine/methanol mixture; polarized Raman study; Raman line shape analysis; DFT calculations

Introduction

Hydrogen bonding plays a central role in the structure and function of biological systems.[1–3] Spectroscopic studies of weakly bound intermolecular complexes have provided a wealth of information on the structure and dynamics of such species[4] and define a starting point for a detailed understanding of various macroscopic phenomena. An important area in the study of intermolecular interactions is that of aromatic compounds in both gas and condensed phases. The application of spectroscopic techniques in such studies was reviewed by Zwier[5] almost a decade ago. It is amply clear from this review that there are a large number of systems that can be studied by employing a variety of experimental techniques. It is, therefore, quite important to select such systems that can serve as useful prototypes of important and unique properties.

The experimental study of hydrogen-bonded binary mixtures by Raman spectroscopy increases our understanding of intermolecular interactions. The analysis of the line profiles and wavenumber shifts of selected vibrational Raman bands allows studying inter- and intramolecular interactions as well as molecular reorientations. Asthana and Kiefer[6] have presented a comprehensive review on this subject. In contrast to the wavenumber position of a Raman band, which relates to the corresponding force constant basically depending on the electronic structure and bonding, the Raman line width contains useful information on the dynamical aspects of the picosecond to sub-picosecond timescale in molecular liquids and solids: for instance, regarding vibrational relaxation (dephasing) and reorientational motions.[7] An obvious advantage of Raman spectroscopy over infrared (IR) spectroscopy, i.e. the separation of vibrational and reorientational contributions to the line shape of a vibrational Raman band, was recognized quite early by Bartoli and Litovitz.[8]

Pyrimidine (Pd) is the parent heterocyclic of a very important group of compounds that have been studied extensively because of their occurrence in living systems.[9,10] Pyrimidine and its derivatives possess remarkable biological activity and they have been used widely in the fields ranging from medicinal to industrial applications. The pyrimidine ring system provides a potential binding site for metals and hence any information on their coordinating property is important for understanding the role of metal ions in biological systems, which are extremely vital for many life processes. The interpretation of vibrational spectroscopic data in liquid phase, in conjunction with an

* *Correspondence to: B. P. Asthana and Ranjan K. Singh, Department of Physics, Banaras Hindu University, Varanasi 221005, India. E-mail: bpasthana@rediffmail.com; ranjanksingh65@rediffmail.com*

a *Laser and Spectroscopy Laboratory, Department of Physics, Banaras Hindu University, Varanasi 221005, India*

b *Department of Physics, Motilal Nehru National Institute of Technology, Allahabad 211004, India*

c *Fachbereich Physik, Universität Osnabrück, D-49076 Osnabrück, Germany*

d *Institut für Physikalische Chemie, Friedrich-Schiller Universität Jena, D-07743 Jena, Germany*

appropriate theoretical model, can provide quite important clues for interpreting the experimentally observed spectral features in terms of explicit molecular structures present in the liquid. In this respect, quantum chemical approach including density functional theory (DFT) have contributed to our understanding of the hydrogen bond.[11,12] Several binary ionic complexes of small organic molecules with hydrogen donor solvents have been examined recently.[1,13–17] Balci and Akyuz[18] reported recently a detailed theoretical vibrational spectroscopic study of free 4-aminopyrimidine molecule using DFT calculations. In this study, a detailed investigation of the geometrical structure, force field, electro-optical parameters, relative IR intensities and harmonic vibrational wavenumbers of free 4-aminopyrimidine molecule in the electronic ground state was carried out. Melandri *et al.*[19] reported experimental and theoretical results on the 1 : 1 complex of pyrimidine and water. In this study millimeter-wave and microwave absorption, and Fourier transform spectra of the 1 : 1 complex between pyrimidine and four isotopomers of water (H_2O, HDO, D_2O and $H_2{}^{18}O$) were investigated. Recently, another Raman spectroscopic study of the two-dimensional polymer compound of 2-aminopyrimidine was made by Akyuz and Akyuz.[20] A spectroscopic study of molecular interactions of harmane with pyrimidine and other diazens was reported in an earlier work.[21] Recently, a study of the first singlet excited state of hydrogen-bonded complexes between pyrimidine and water was reported.[22] These studies lead to an improved understanding of the spectroscopy of pyrimidine in liquid water. In yet another recent study, hydrogen bonding in a pyrimidine containing macrocycle was reported.[23]

The most recent study on hydrogen-bonded complexes of pyrimidine with water has been performed by Schlücker *et al.*[24] Polarization-resolved Raman spectra and DFT calculations on the hydrogen bonding between pyrimidine and water was reported with different mixture compositions. In the present study, methanol (M) was chosen as a protic solvent, which acts as an H-bond donor. Similar to earlier Raman studies on pyridine[25–28] and pyrimidine,[24] the ring-breathing mode ν_1 of pyrimidine at *ca* 990 cm^{-1} was chosen as the marker band. The ring-breathing vibration ν_1 is well known to be sensitive to hydrogen bonding between nitrogen-containing heterocyclic group and a hydrogen donor solvent.[24–26,28–32] Our vibrational spectroscopic analysis on hydrogen bonding between pyrimidine and methanol comprises both experimental Raman spectra and DFT calculations on structures and vibrational spectra of various Pd/M complexes with varying solvent content.

Methods

Experimental techniques

Commercially obtained pyrimidine was used without further purification. The parallel ($I_{||}$) and perpendicular ($I_{\perp}$) components of the Raman scattered intensity were recorded in the 970–1020 cm^{-1} region for neat Pd and Pd/M mixtures with mole fractions of Pd ranging from $x(Pd) = 0.01$ to 1.00 at 28 different mole fractions of the reference system Pd. The 514.5 nm line of an Ar^+ laser which delivered 100 mW power at the sample was used for excitation. The Raman signal was collected using the 90° scattering geometry. A double monochromator (Spex 1404) with 2400 grooves/mm gratings and a liquid-N_2-cooled charge-coupled device detector (Photometrics) were employed to record the Raman spectra. The high spectral resolution of approximately 0.36 cm^{-1}, equivalent to an entrance slit width of 50 μm, allows the determination of peak positions and line widths with high precision. For all measurements, the grating position was kept constant, which ensured reproducibility and a reasonably high precision in the determination of peak positions. The $I_{||}$ and $I_{\perp}$ components of the Raman scattered intensity were measured for each binary mixture by turning the polarization of the incident laser beam by 90° using a double Fresnel rhomb before the sample; the analyzer position was kept constant to avoid any errors that might creep in due to the polarization dependency of the detection system.

Computational methods

The ground state geometries and vibrational spectra for free Pd (pd) and its hydrogen-bonded complexes with one up to four molecules of methanol were optimized by using Becke's three-parameter exchange function (B3)[33] in combination with the LYP correlation functions of Lee *et al.*,[34] and the 6-311++G(d,p) basis set with polarization and diffuse functions. Calculations were performed with the GAUSSIAN 03 suite of programs.[35] Internal coordinates were generated using the software GAUSS VIEW[36] by starting initially from pd species and then successively adding methanol molecules to it. In order to account for the solvent methanol, the vibrational wavenumber for the ring-breathing mode of pyrimidine was calculated using integral equation formalism polarizable continuum model (IEF-PCM) solvation model.[37] The results are reported in Table 1. In addition to applying the solvation model for pyrimidine, vibrational wavenumbers were also calculated for two more Pd_xM_y clusters, PdM and $PdM_{2(1+1)}$, using the specific bulk solvent effect (IEF-PCM). The results are also reported in Table 1. However, the wavenumber values differ by hardly ~1 cm^{-1} in these two cases also as compared to the gas-phase results. Hence the bulk solvent effect calculations were not performed for other clusters.

DFT Calculations on Pyrimidine/Methanol Complexes

In the binary system Pd/M, many different hydrogen-bonded complexes can be simultaneously present. The two nitrogen atoms of Pd are potential hydrogen-acceptor sites. We therefore calculated the structures and the vibrational spectra of various small Pd_xM_y clusters with stoichiometric ratios $x : y$ ranging from 2 : 1 to 1 : 4.

Table 1. N···H bond distances and vibrational wavenumbers of the ring-breathing mode ν_1 for neat Pd and different hydrogen-bonded Pd_xM_y clusters

Complex	Relative energy (kJ/mol)	$d(N_1\cdots H)$ (A°)	$d(N_2\cdots H)$ (A°)	ν_1 (cm^{-1})	ν_1 (cm^{-1}) (solvation)
Pd	–	–	–	1011.2	1012.4
Pd_2M	–	1.93	–	1018.7	–
PdM	–	1.97	–	1018.5	1019.8
$PdM_{2(2+0)}$	0	1.89	–	1020.2	–
$PdM_{2(1+1)}$	+14.2	1.99	1.99	1024.9	1025.7
$PdM_{3(3+0)}$	0	1.86	–	1021.3	–
$PdM_{3(2+1)}$	+14.4	1.92	1.98	1026.4	–
$PdM_{4(3+1)}$	+2.4	1.87	1.98	1027.5	–
$PdM_{4(2+2)}$	0	1.90	1.90	1027.7	–

Journal of RAMAN SPECTROSCOPY

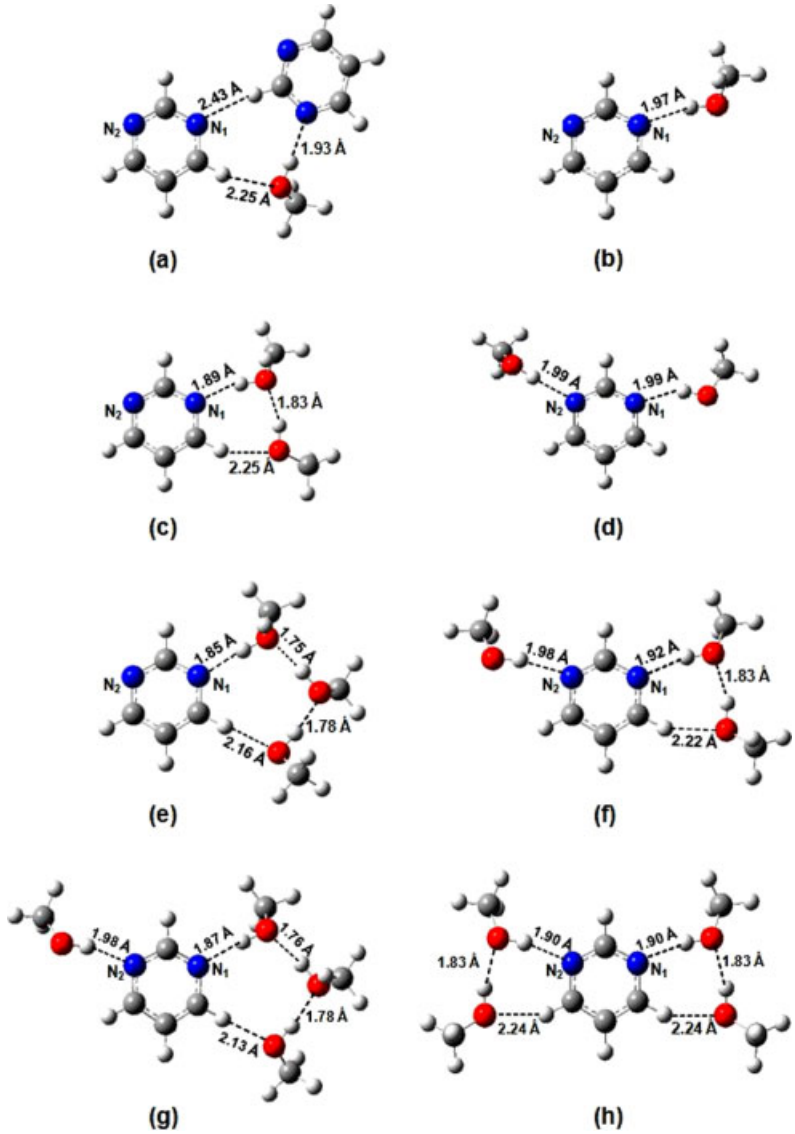

Figure 1. Optimized geometries of various hydrogen-bonded Pd_xM_y clusters: (a) Pd_2M; (b) PdM; (c) $PdM_{2(2+0)}$; (d) $PdM_{2(1+1)}$; (e) $PdM_{3(3+0)}$; (f) $PdM_{3(2+1)}$; (g) $PdM_{4(3+1)}$ and (h) $PdM_{4(2+2)}$.

Structures and N···H bond distances

The structures of the 2:1 (Pd_2M) to 1:4 (PdM_4) clusters are presented in Fig. 1. In the 2:1 (Pd_2M) complex, the two Pd rings lie in nearly the same plane, but oriented with respect to each other, which is significantly different from what was obtained in the earlier study[24] on pyridine/water (Pd/W), where the two Pd rings were in perpendicular orientation. In the Pd_2M complex, only one N atom of the Pd ring is attached to the H atom of the solvent molecule, whereas the other Pd ring is attached to the O atom of the OH group of the solvent (M). It is to be noted that, in the case of Pd/W, only two hydrogen bonds are formed and both bonds are equivalent since the two Pd rings are connected to the H atom of the water molecule symmetrically through N atom of the Pd ring. However, in the present study on Pd/M, a closed network of three hydrogen bonds is formed (Fig. 1(a)). Furthermore, the hydrogen bond between the N atom of the Pd ring and the H atom of the OH group of the solvent in Pd_2M is much stronger (1.93 Å) and more linear, whereas this bond was much weaker (2.04 Å) and relatively less linear in the case of Pd_2W complex studied earlier.[24] The 1:1 (Pd/M) complex depicted in Fig. 1(b) exhibits a hydrogen-bond length of 1.97 Å, which is slightly longer, and therefore weaker, compared to that in the Pd_2M complex. It is also supported by the fact that the hydrogen bond is more linear in the case of Pd_2M having the inter-bond angle N···H–O ≈ 176°, whereas the corresponding angle in PdM is *ca* 166°.

Hydrogen bonding of two methanol molecules to a single Pd molecule may lead to complexes, such as $PdM_{2(2+0)}$ or $PdM_{2(1+1)}$ clusters shown in Fig. 1(c) and (d), respectively. In the $PdM_{2(2+0)}$ complex, the N···H bond length is 1.89 Å and it is stronger compared to the corresponding hydrogen bonds in the Pd_2M and PdM complexes. It is further to be noted that, in case of $PdM_{2(2+0)}$ complex, a strong hydrogen bond (1.83 Å) is formed between the two methanol molecules. In contrast to the $PdM_{2(2+0)}$ cluster, in the $PdM_{2(1+1)}$ cluster, Pd is symmetrically complexated by two methanol molecules and N···H bond length is 1.99 Å for both the hydrogen-bonding sites. This indicates that the strength of both the hydrogen bonds in $PdM_{2(1+1)}$ is close to that in the 1:1 Pd/M complex.

Similar to the 1 : 2 stoichiometry, hydrogen bonding of three methanol molecules to Pd can result in the formation of the two PdM_3 clusters depicted in Fig. 1(e) and (f). In the complex $PdM_{3(3+0)}$, the arrangement of all three methanol molecules into a single subcluster causes a significant N···H bond contraction to 1.85 Å as compared to 1.89 Å for the $PdM_{2(2+0)}$ complex, and the angle N···H–O in the $PdM_{3(3+0)}$ cluster is 176°, which is larger than the corresponding angle (166.5°) in the cluster $PdM_{2(2+0)}$. These data also, therefore, support the fact that, due to the higher linearity, the N···H hydrogen bond is stronger in case of $PdM_{3(3+0)}$ as compared to that in the $PdM_{2(2+0)}$ cluster. Thus, an increasing number in the cluster leads to stronger interactions and a shorter N···H hydrogen bond. Apart from the $PdM_{3(3+0)}$, a $PdM_{3(2+1)}$ complex can also be formed by adding a third methanol molecule to the $PdM_{2(1+1)}$ cluster. In the $PdM_{3(2+1)}$ complex, the second N···H bond is reduced further and assumes a value of 1.91 Å as compared to 1.99 Å in the case of the $PdM_{2(1+1)}$ complex.

The structures of two distinct 1 : 4 (PdM_4) clusters are shown in Fig. 1(g) and (h). Our calculations are restricted to species with a maximum of three methanol molecules (M_3 subcluster) attached to one N atom of Pd having overall a maximum of four methanol molecules. The other possibility is that, when we add a methanol molecule to the $PdM_{3(2+1)}$, the species $PdM_{4(2+2)}$ is formed. The hydrogen bond N···H distance reduces to 1.90 Å in the $PdM_{4(2+2)}$ cluster in comparison to 1.98 in the $PdM_{3(2+1)}$ cluster. The species $PdM_{4(2+2)}$ shows a symmetric hydrogen bond to both the N atoms of the Pd ring and on each side, the hydrogen bond distance N···H is 1.90 Å and the O···H hydrogen bond distance in the methanol–methanol network is 1.83 Å (Fig. 1(h)). It is interesting to note that in all the three species $PdM_{2(2+0)}$, $PdM_{3(2+1)}$ and $PdM_{4(2+2)}$, in which two methanol molecules are attached on one side of the Pd ring, the hydrogen-bond length in the methanol–methanol network is always 1.83 Å. When we add a further methanol molecule to the species $PdM_{3(2+1)}$, it forms the $PdM_{4(3+1)}$ species. A strong hydrogen bond occurs in $PdM_{4(3+1)}$ and the N···H bond distance is 1.87 Å in comparison to 1.91 Å in the case of $PdM_{3(2+1)}$ cluster. It is quite interesting to note that the O···H hydrogen bonds between methanol molecules are much stronger (1.76 and 1.78 Å) than the hydrogen bond formed by the O atom of the last methanol molecule to the H atom of the Pd ring, which forms a much weaker hydrogen bond having O···H bond length of 2.13 Å (Fig. 1(g)).

Relative stability of Pd_xM_y clusters

Table 1 contains the relative energies for pairs of Pd_xM_y cluster with the same number of methanol molecules. The hydrogen-bonded distances (N···H) and vibrational wavenumbers for the Pd ring-breathing mode ν_1 for all complexes are also listed in Table 1. In general, the clusters in which all methanol molecules are attached to one side of the Pd ring are more stable. For example, the complex $PdM_{2(2+0)}$ is 14.2 kJ/mol more stable than the $PdM_{2(1+1)}$ species. Similarly, the $PdM_{3(3+0)}$ complex is 14.4 kJ/mol more stable than $PdM_{3(2+1)}$. For $PdM_{4(2+2)}$ and $PdM_{4(3+1)}$, however, the difference is only 2.4 kJ/mol, which essentially means that the two clusters are almost equally stable.

Wavenumber shifts of the ν_1 ring (Pd) breathing mode upon complexation

In the present study, the Raman peak position of the Pd ring-breathing mode ν_1 was chosen for monitoring the degree of hydrogen bonding between pyrimidine and methanol molecules. For this purpose, we calculated the vibrational wavenumbers of the different Pd_xM_y clusters depicted in Fig. 1. The corresponding (unscaled) harmonic wavenumbers of the ν_1 mode of all possible Pd_xM_y clusters are presented in Table 1. The wavenumber values for ν_1 differ by approximately 16 cm^{-1} and increase from 1011.2 cm^{-1} for neat Pd to 1027.7 cm^{-1} for $PdM_{4(2+2)}$. At a first glance, one may observe a positive correlation of ν_1 (Pd) with the Pd/M stoichiometry: for instance, 1.97 Å for PdM to 1.86 Å for PdM_3; the ν_1 (Pd) values for clusters with the same stoichiometric Pd/M ratio are 1018.5 cm^{-1} for $PdM_{1(1+0)}$, 1020.2 cm^{-1} for $PdM_{2(2+0)}$ and 1021.3 cm^{-1} for $PdM_{3(3+0)}$. In these Pd/M complexes, a systematic variation of N···H bond length and ν_1 vibrational wavenumber is observed, which is in close agreement with the results of the earlier study on Pd and water.[24] However, the Pd_2M complex does not follow the trend (Fig. 2), which can be attributed to the fact that the two pyrimidine and one methanol molecules form an asymmetric network, whereas in the case of Pd_2W[24] the two Pd molecules were symmetrically attached to one water molecule. A nitrogen atom of one Pd is directly attached to the H atom of the OH group of CH_3OH, while the other Pd is attached through H atom to the O atom of the CH_3OH molecule. In Pd_2M complex, a deviation from linear correlation between the N···H bond distance and ν_1 (Pd), as depicted in Fig. 2 (lower curve) for the '$x + 0$' series which consists of Pd_2M, PdM, $PdM_{2(2+0)}$ and $PdM_{3(3+0)}$, is therefore not unexpected.

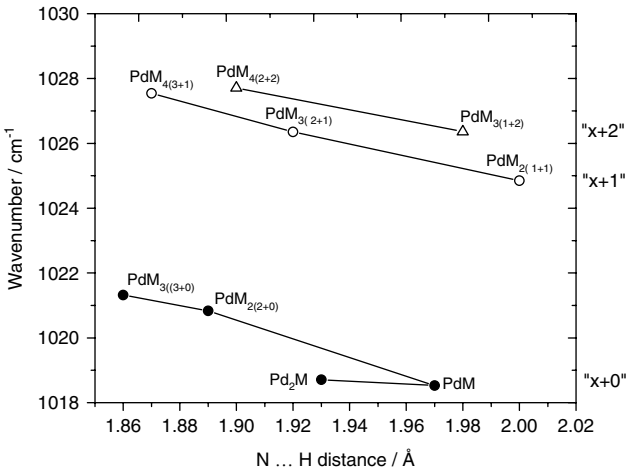

Figure 2. Correlation of calculated ν_1 wavenumbers (Pd) and N···H bond distances for Pd and various hydrogen-bonded Pd_xM_y clusters. Linear correlations are shown for three subgroups of Pd/M complexes, where one hydrogen-bonding site is coordinated to two methanol molecule '$(x + 2)$', one methanol molecule '$(x + 1)$' or no methanol molecule '$(x + 0)$'.

Figure 2 (middle curve) shows the corresponding correlation for the '$x + 1$' series which consists of $PdM_{2(1+1)}$, $PdM_{3(2+1)}$ and $PdM_{4(3+1)}$. In all the structures within this series, an N atom of Pd is attached to the H atom of the OH group of one methanol: N_1···H bond lengths being *ca* 1.99, 1.92 and 1.87 Å, respectively. The other methanol molecule is attached always to the other N atom of Pd, and the N_2···H bond lengths remain almost constant, 1.99, 1.98 and 1.98 Å in $PdM_{2(1+1)}$, $PdM_{3(2+1)}$ and $PdM_{4(3+1)}$, respectively. The regression lines for these two subgroups, series '$x+0$' and '$x+1$' are separated by ~6 cm^{-1}, except for Pd_2M. This is an indication of the fact that wavenumber shifts induced by the methanol molecule follow a regular trend for both subgroups.

Journal of RAMAN SPECTROSCOPY

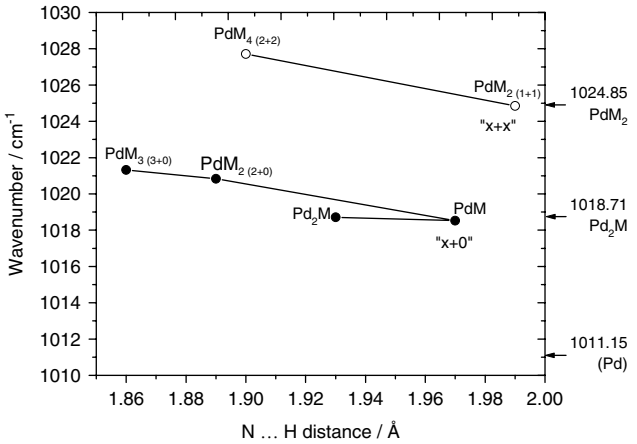

Figure 3. Correlation of calculated ν_1 wavenumbers (Pd) and N···H bond distances. Linear correlations are shown for a series of complexes, where one hydrogen-bonding site '$(x + 0)$' or both binding sites '$(x + x)$' of Pd are successively coordinated by methanol molecules.

A similar behavior is observed for the '$x + 2$' series also (Fig. 2, upper curve). The effect of adding two methanol molecules, one to each N atom of Pd, is depicted in Fig. 3 (upper curve). This subgroup is labeled as '$x + x$' and contains the clusters $PdM_{2(1+1)}$ and $PdM_{4(2+2)}$; the regression lines for the '$x + 0$' and '$x + x$' subgroups are also separated by approximately 6 cm^{-1} and their slopes are also quite similar. A comparison between the two subgroups is depicted in Fig. 3. These results clearly suggest that, by adding two methanol molecules, one molecule to one N atom and the other molecule to the other N atom of Pd simultaneously, the induced wavenumber shift is nearly the same as by adding one methanol, while in the study of Pd/W complex[24] when two water molecules are added simultaneously instead of one, the induced wavenumber shift is doubled and the regression line for the '$x + x$' series has a slope which is two times the slope for the '$x + 0$' series. The calculated wavenumber ν_1 for free Pd (pd) is 1011.15 cm^{-1} (Fig. 3, bottom right). Thus, pd as the only non-hydrogen-bonded species is spectrally clearly separated from all other hydrogen-bonded complexes, the difference from the lowest wavenumber of '$x + 1$' series being approximately 7 cm^{-1} (Table 1).

Polarized Raman Spectroscopy

The parallel ($I_{||}$) and perpendicular ($I_{\perp}$) components of the Raman spectra of neat Pd and 27 binary mixtures ($C_4H_4N_2$ + CH_3OH) Pd/M with mole fractions of the reference system Pd ranging from x(Pd) = 1.00 to 0.01 were recorded in the region 970–1020 cm^{-1}. The experimentally measured parallel ($I_{||}$) and perpendicular ($I_{\perp}$) components of the Raman scattered intensity were used to obtain the isotropic part of the Raman spectra at each concentration by making a linear combination of $I_{||}$ and $I_{\perp}$ employing the relationship[6,8]:

$$I_{iso} = I_{||} - 4/3\, I_{\perp} \quad (1)$$

The isotropic parts of the Raman spectra thus obtained for the neat Pd as well as eight other concentrations of the reference system in the binary mixture are depicted in Fig. 4. Neat Pd (Fig. 4, top) shows a band at 990.0 cm^{-1}, which is assigned to the ring-breathing mode ν_1. The addition of CH_3OH (M) yields a new broad band at ≈994.5–996.2 cm^{-1} on going from mole fraction x(pd) = 0.85 to 0.05, as shown in Fig. 4. Upon addition of the solvent

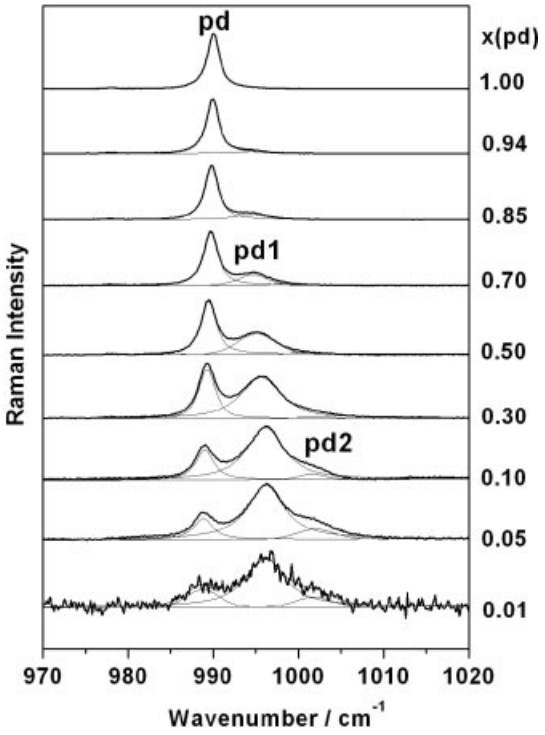

Figure 4. Isotropic components of the Raman spectra of neat Pd and Pd/M mixtures with different Pd mole fractions x(pd), along with the analyzed component bands shown by dotted lines.

CH_3OH, a new band at 994.2 cm^{-1} appears at x(pd) = 0.96 (not shown in Fig. 4). This new band is obviously due to the formation of a hydrogen-bonded species, in particular Pd_2M. As can be seen from the Raman spectra for x(pd) = 0.85 and 0.70 depicted in Fig. 4, both the relative intensity and the wavenumber of this additional Raman band increase. For x(pd) = 0.85, 0.70, 0.50, 0.30, 0.10 and 0.05, a line shape analysis of the band envelope suggests the presence of three distinct spectral components at high dilutions. Hydrogen-bonded species pd_1 are observed from x(pd) = 0.96 to 0.01, whereas the pd_2 species are observed from x(pd) = 0.75 to 0.01. At very high dilutions, i.e. x(pd) = 0.10 and 0.05 (Fig. 4, second and third spectra from the bottom), the contributions of the hydrogen-bonded species dominate over the pd species. Both the relative intensity and the wavenumber for the hydrogen-bonded species increase as compared to the neat Pd, while in the earlier study on Pd/W by Schlücker *et al.*,[24] it was observed that at high dilutions, such as x(pd) = 0.10 and 0.05, contributions of only hydrogen-bonded species were observed and the ν_1 mode of free Pd vanished almost completely at these high dilutions.

Decomposition of isotropic Raman component

In order to examine the trend of the concentration-dependent variation, a decomposition of the band envelope of the isotropic Raman spectra was performed for each mixture composition. The decomposed Raman band along with the component bands for neat Pd and eight other mole fractions, x(pd) = 0.94, 0.85, 0.70, 0.50, 0.30, 0.10, 0.05 and 0.01, are also depicted in Fig. 4. For mole fractions x(pd) = 0.96–0.79, the overall band profile was fitted to two Voigt profiles because of the existence of two chemically distinct hydrogen-bonded species. The decomposed Raman data are presented in Table 2. In order to ensure that the

Table 2. Wavenumbers (cm^{-1}) of the ring-breathing mode ν_1 of pd (free pyrimidine), pd1 and pd2 (hydrogen-bonded pyrimidine) obtained by the line shape analysis of the experimentally measured Raman spectra as a function of pyrimidine mole fraction in Pd/M mixtures

Species	pd	pd1	pd2		pd	pd1	pd2
x(pd)	Wavenumber (cm^{-1})			x(pd)	Wavenumber (cm^{-1})		
1.00	990.04	–	–	0.64	989.69	994.94	1000.83
0.98	990.00	–	–	0.60	989.62	994.94	1000.49
0.96	989.97	994.19	–	0.54	989.55	995.06	1000.90
0.94	989.97	994.44	–	0.50	989.49	995.15	1000.94
0.93	989.94	994.37	–	0.44	989.43	995.26	1001.24
0.91	989.91	994.44	–	0.39	989.39	995.37	1001.66
0.89	989.90	994.46	–	0.33	989.34	995.54	1001.76
0.88	989.89	994.47	–	0.30	989.30	995.66	1002.13
0.86	989.85	994.50	–	0.24	989.26	995.82	1002.08
0.85	989.84	994.50	–	0.20	989.20	995.93	1002.11
0.83	989.81	994.50	–	0.13	989.11	996.10	1001.60
0.79	989.81	994.57	–	0.10	989.03	996.17	1001.64
0.75	989.76	994.67	999.49	0.05	988.86	996.21	1002.02
0.70	989.73	994.80	1000.34	–	–	–	–

components obtained were not an artifact of the fitting routine, a number of widely varying preliminary guesses were made for the peak position and the line width of both the components, but the analysis always yielded finally the same peak position and line width of both the components with each initial guess. This was done in order to ascertain that the fitting procedure is working in this case fairly consistently. At x(pd) = 0.70 (Fig. 4), a weak third band at 1000.3 cm^{-1} is observed clearly in the Raman spectrum. This new band is assigned to ν_1 mode of the hydrogen-bonded complexes of Pd when overall large methanol content is present. Three component bands were obtained using the above-mentioned fitting procedure for mole fractions x(pd) = 0.75–0.01. The isotropic part of the Raman spectra for x(pd) = 0.30, 0.10 and 0.05 depicted in Fig. 4 clearly indicate the coexistence of two hydrogen-bonded and one non-hydrogen-bonded Pd species. At x(pd) = 0.30, the intensity of the hydrogen-bonded component is somewhat weak, but at x(pd) = 0.20 and 0.05 the wavenumber positions and the corresponding integrated intensity ratios of the bands corresponding to the hydrogen-bonded species to free Pd are quite large. In the study of Pd/W by Schlücker *et al.*,[24] for mole fraction 0.10 and below, the amount of non-hydrogen-bonded or free Pd was almost negligible and only two Voigt profiles due to hydrogen-bonded species were considered, while in the present work on Pd/M, even at sufficiently high dilutions (below mole fraction 0.10) the peak corresponding to the non-hydrogen-bonded species has a noticeable intensity, which essentially means that some free Pd molecule are still present.

In order to understand the above-mentioned difference between Pd/W and Pd/M systems, as evident from their spectra, especially at low mole fraction (<0.1) of Pd, apart from the broad guidelines derived from the work of Fileti *et al.*,[38] several other factors seem to be responsible. Firstly, regarding the strength of hydrogen bond interaction, going by bulk property, one can recall that the boiling point of water (100 °C) is higher than the boiling point of methanol (87 °C). This shows that intermolecular hydrogen bond interaction in water is stronger than that in methanol. However, this aspect based on a bulk property alone is not sufficient to explain the observed spectral difference between Pd/W and Pd/M systems and other molecular-level effects need to be considered. A second very important aspect, which needs to be considered, is the fact that water molecule can form two hydrogen bonds, whereas methanol molecule can form only one hydrogen bond. It is obvious that at same molar concentration, more number of Pd molecules is likely to be consumed in case of Pd/W system than that in the case of Pd/M system. This may eventually lead to a drastic reduction in the intensity of the Raman peak corresponding to pd species in the Pd/W system, whereas it may appear with significant intensity in the case of Pd/M system. The steric hindrance in complex formation is obviously much more in case of Pd/M complexes than in the case of Pd/W complexes and this may also lead to an appreciable intensity of the Raman peak corresponding to pd species in case of Pd/M system.

Furthermore, in their study on electronic charges due to thermal disorder of hydrogen bonds in liquid, Fileti *et al.*[38] have pointed out that the proton accepter site of a solute molecule experiences a great local thermal disorder in an aqueous environment. The hydrogen bonds lead to a local change in the electronic environment and thereby affect the atomic charges, dipole moment and dipole polarizability. It has been estimated in this study that, on average, pyridine transfers – 0.036 ± 0.015 elementary charge to the water molecule when different pyridine/water clusters are formed. Murray *et al.*[39] also studied the pyridazine + H_2O/D_2O system experimentally as well as theoretically using DFT method and found out that there is a net charge transfer from pyridazine to H_2O/D_2O and one pyridazine attaches to itself on average 3.5 water molecules. Keeping in view the results from these two studies,[38,39] we performed DFT calculations on different Pd_xW_y and Pd_xM_y clusters and analyzed the data on charge transfer from Pd to the solvent water/methanol. It was quite evident form these results that, in general, for the clusters with same stoichiometric ratio, the required charge transfer for the hydrogen-bond formation is far greater in case of Pd/M system (e.g. 0.105e for $PdM_{3(2+1)}$ cluster) than in the case of corresponding $PdW_{3(2+1)}$ cluster (0.042e). Thus, Pd_xW_y clusters require less transfer of charge than the Pd_xM_y clusters. This essentially means that the formation of Pd_xW_y clusters is much easier than that of Pd_xM_y clusters. Thus it is most likely that at very high dilutions (<0.1) almost all Pd molecules are consumed in forming hydrogen-bonded complexes in Pd/W system, whereas a significant number of free Pd molecules are present in the case Pd/M system and thereby resulting in a significant intensity of the Raman peak corresponding to pd species.

Line shape analysis: wavenumber shift and line width change

The wavenumbers of the ring mode ν_1 in the three different species pd, pd1 and pd2 depending on mixture composition ranging from x(pd) = 1 to 0.05 are listed in Table 2 and presented in Fig. 5 as a function of concentration, x(pd). Our interpretation of the observed concentration dependence of ν_1 in a particular species is based on the postulation that this mode explores the substance composition in terms of different species and, to a definite extent, the interaction with the environment. The line width (full width at half-maximum (FWHM)) of the ring-breathing mode ν_1 of Pd also presents three distinct species, pd, pd1 and pd2, depending on the mixture composition ranging from x(pd) = 0.05 to 1.0 as listed in Table 3 and presented in Fig. 6. The analysis of the concentration dependence of the line width is capable of probing dynamic processes, such as concentration fluctuations,[40]

Journal of RAMAN SPECTROSCOPY

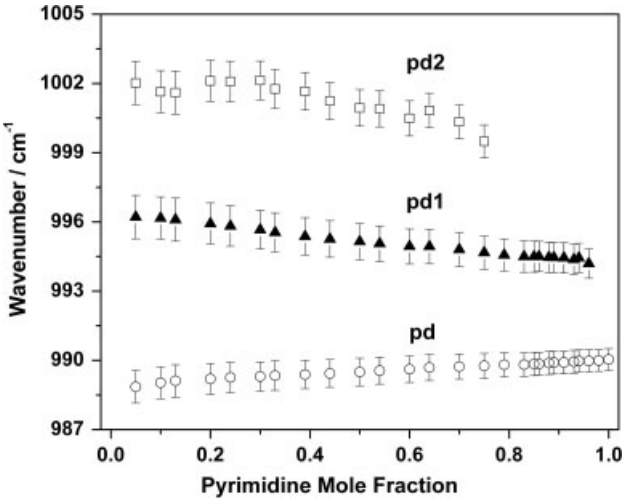

Figure 5. Concentration dependence of the ν_1 wavenumbers (Pd) for the non-hydrogen-bonded species pd and the two hydrogen-bonded species pd1 and pd2.

Table 3. Line widths (FWHM in cm^{-1}) of the ring-breathing mode ν_1 of pd (free pyrimidine), pd1 and pd2 (hydrogen-bonded pyrimidine) obtained by the line shape analysis of the experimentally measured Raman spectra as a function of pyrimidine mole fraction in Pd/M mixtures

Species	pd	pd1	pd2		pd	pd1	pd2
x(pd)	Line width ($\Delta\tilde{\nu}_{1/2}$/cm^{-1})			x(pd)	Line width ($\Delta\tilde{\nu}_{1/2}$/cm^{-1})		
1.00	1.734	–	–	0.64	2.081	5.197	3.258
0.98	1.741	–	–	0.60	2.120	5.097	3.725
0.96	1.768	3.209	–	0.54	2.150	5.332	3.621
0.94	1.762	3.495	–	0.50	2.201	5.392	3.781
0.93	1.819	3.690	–	0.44	2.214	5.536	2.753
0.91	1.835	3.848	–	0.39	2.261	5.636	3.000
0.89	1.837	4.217	–	0.33	2.357	5.675	3.898
0.88	1.835	4.228	–	0.30	2.337	5.811	3.710
0.86	1.830	4.331	–	0.24	2.452	5.753	4.000
0.85	1.870	4.530	–	0.20	2.472	5.684	3.810
0.83	1.898	4.486	–	0.13	2.597	5.463	3.050
0.79	1.926	4.754	–	0.10	2.544	5.270	3.270
0.75	1.984	4.611	3.527	0.05	2.604	5.119	5.305
0.70	2.016	4.965	3.640	–	–	–	–

diffusion of the solvent into the reference system,[41] variation of the mixture microviscosity with concentration,[42] etc.

The increase in the line width on increasing the solvent concentration can be explained in terms of two factors: the coexistence of various clusters, and the statistical distribution of the hydrogen bond strength owing to the shallow potential well for the hydrogen bond. Various Pd/M clusters exist simultaneously in solution and contribute to the line width. From the experimental data, we found that pd, pd1 and pd2 coexist in the mixture, at least for intermediate concentrations. A band decomposition into the contributions from the three species (pd, pd1 and pd2) allows one to separately analyze both peak wavenumbers and line widths. The line widths corresponding to the spectral components of the species pd1 and pd2 are significantly larger compared to pd due to hydrogen bonding (Table 3 and Fig. 6).

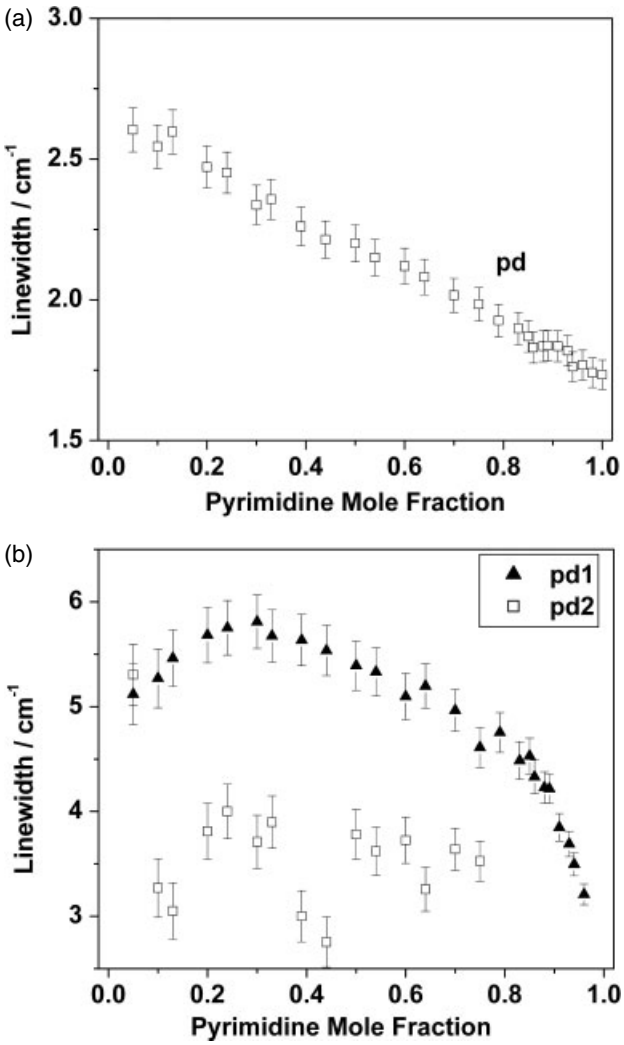

Figure 6. (a) Concentration dependence of the ν_1 line width (Pd) for 'free' Pd. (b) Concentration dependence of the ν_1 line width (Pd) for the hydrogen-bonded species pd1 and pd2.

Non-hydrogen-bonded or free Pd species (pd)

It is obvious from the data presented in Table 2 and also in Fig. 5 (bottom curve) that the non-hydrogen-bonded species, pd, shows a small red shift upon dilution. In going from neat Pd to binary mixture, pd shows a continuous decrease with dilution although the variation of wavenumber with concentration is small and it is downshifted from 990.0 cm^{-1} at x(pd) = 1.0 to 988.9 cm^{-1} at x(pd) = 0.05 and the entire shift is only around 1.1 cm^{-1}. It is evident from the variation of wavenumber of pd with concentration depicted in Fig. 5 (bottom curve) that there is an appreciable drop in the wavenumber of free pd in going from x(pd) = 0.20 to 0.05. The observed small negative wavenumber shift of pd is probably due to increased interaction between Pd and its environment as the dilution of the mixture increases. This is attributed to the fact that either the hydrogen-bonded species or methanol clusters induce a very small reduction of the electron density on the Pd ring, which causes a slightly smaller force constant for the ν_1 (pd) vibration and thereby resulting in a decrease of wavenumber. This postulation is supported by the observation that the line width of the ν_1 (pd) increases linearly from 1.73 to 2.60 cm^{-1} in going from neat Pd to extreme dilution.

Hydrogen-bonded Pd species with low methanol content (pd1)

The concentration-dependent wavenumbers for ν_1 (pd1) are depicted in Fig. 5 (middle curve) and the corresponding values are given in Table 2. It is evident from the data presented in both Table 2 and Fig. 5 that pd1 shows a blue shift upon dilution. On going from neat liquid to very high dilution, pd1 shows a steady increase in wavenumber from 994.2 cm^{-1} at x(pd) = 0.96 to 996.2 cm^{-1} at x(pd) = 0.05. Furthermore, the corresponding line widths show an increase on going from x(pd) = 0.96 to 0.30. However, below x(pd) = 0.30 the line width starts decreasing (Fig. 6(b)). Thus, it is obvious that the concentration fluctuation model of Bondarev and Mardeva,[40] which gives a maximum around x(pd) = 0.50 in the line width *versus* concentration plot, does not seem to be fully operative in this case. The increase in line width up to dilution x(pd) = 0.30 essentially indicates the role of diffusion mechanism in which the solvent molecule, methanol, is diffusing into the reference system. According to the jump diffusion model, a line broadening is caused.[41] It implies that, at high dilution, the number of free pd species is so low that practically there are pd1 oscillators in abundance which experience a collision by all other species present in the mixture. It is quite probable, however, that at high dilution around x(pd) = 0.24, concentration fluctuations[40] may start playing role, which apparently gives a maximum at such a low concentration of the reference system. A shift in the maximum from x(pd) = 0.5 may be explained in terms of our recent model[42] based on microviscosity of the reference system, solvent and the mixture.

Hydrogen-bonded Pd species with high methanol content (pd2)

The concentration dependence of the wavenumber position of ν_1 for the hydrogen-bonded species pd2 is depicted in Fig. 5 (top curve). In comparison to pd and the hydrogen-bonded species pd1, the pd2 species shows a slightly different behavior. The wavenumber and the line width data for the pd2 species with varying concentration are listed in Tables 2 and 3, respectively. At x(pd) = 0.75, the first mixture concentration for which the pd2 species is observed upon dilution, the wavenumber of ν_1 (pd2) is 999.5 cm^{-1}. A nearly linear increase of ν_1 (pd2) in the mole fraction range x(pd) = 0.70 to 0.50 is observed (Fig. 5), which clearly tells that the degree of hydrogen bonding in terms of multiple hydrogen-bonded molecules is increasing. In the mole fraction range x(pd) = 0.50 to 0.20, the ν_1 (pd2) shows an appreciable increment (1.2 cm^{-1}). After reaching the maximum value at x(pd) = 0.20, the ν_1 (pd2) starts slightly decreasing. The corresponding line width data presented in Table 3 reveal that the line width variation with concentration for the pd2 species does not follow any regular trend except for the fact that the line widths are relatively large at intermediate concentrations.

Conclusions

Hydrogen bonding between the H-acceptor pyrimidine and the H-donor methanol was investigated by Raman spectroscopy and DFT calculations. Structures and vibrational wavenumbers for neat Pd and eight hydrogen-bonded Pd/M complexes with different stoichiometric ratios were calculated employing DFT at the B3LYP/6-311++G(d,p) level of theory. Our calculations lead to two major results from Raman experiments on Pd/M complexes; the resolution of different hydrogen-bonded species is possible because of their distinct wavenumber positions, and the shift of ν_1 wavenumbers can be explained by the presence of different Pd/M clusters with varying contributions as a function of mixture composition. Specifically, the isotropic components of the Raman spectra show three distinct contributions in the region 970–1020 cm^{-1}, which are attributed to free pyrimidine, pd, and two hydrogen-bonded species, pd1 and pd2, corresponding to low methanol content and high methanol content, respectively. Finally, a spectra–structure correlation for different cluster subgroups was obtained.

Acknowledgements

The authors are thankful to Prof. W. Kiefer, University of Würzburg, for providing access to his laboratories, for initiating the authors in to this field and also for his many valuable suggestions. Two of us (DKS and SM) are thankful to U.G.C, New Delhi, for the award of a 'Research Fellowship in Science for Meritorious Students' (RFSMS). Four of us (BPA, RKS, AKO and SKS) thank the Alexander von Humboldt-Stiftung, Germany, for financial support in one form or the other. RKS is thankful to DST, India, for financial support. The financial support received under 'DST-DAAD PPP' is also gratefully acknowledged.

References

[1] P. R. Rablen, J. W. Lockman, W. L. Jorgensen, *J. Phys. Chem. A* **1998**, *102*, 3782.
[2] G. A. Jeffrey, W. Saenger, *Hydrogen Bonding in Biological Structure*, Springer-Verlag: Berlin, **1991**.
[3] E. N. Baker, R. E. Hubbard, *Prog. Biophys. Mol. Biol.* **1984**, *44*, 97.
[4] P. Hobza, R. Zahradnik, *Intermolecular Complexes*, Academia: Prague, **1988**.
[5] T. S. Zwier, *Annu. Rev. Phys. Chem.* **1996**, *47*, 205.
[6] B. P. Asthana, W. Kiefer, *Vibrational Spectra and Structure*, vol 20, (Ed. J. R. During), Elsevier: Amsterdam, **1992**, pp 67.
[7] W. G. Rothschild, *Dynamics of Molecular Liquids*, Wiley: New York, **1983**.
[8] F. J. Bartoli, T. A. Litovitz, *J. Chem. Phys.* **1972**, *56*, 404.
[9] R. K. Murray, D. K. Granner, P. A. Mayes, V. W. Rodwell, *Harpers Biochemistry* (22th edn), Prentice Hall International Inc.: London, **1990**.
[10] S. N. Pandeya, D. Sriram, G. Nath, E. De. Clercq, *IL Farmaco* **1999**, *54*, 624.
[11] M. S. Gordon, J. H. Jensen, *Acc. Chem. Res.* **1996**, *29*, 536.
[12] S. Schlund, C. Schmuck, B. J. Engels, *J. Am. Chem. Soc.* **2005**, *127*, 11115.
[13] L. C. Remer, J. H. Jensen, *J. Phys. Chem. A* **2000**, *104*, 9266.
[14] A. T. Pudzianowski, *J. Phys. Chem.* **1996**, *100*, 4781.
[15] P. K. Sahu, A. Chaudhari, S. Long Lee, *Chem. Phys. Lett.* **2004**, *386*, 351.
[16] C. Tuma, A. D. Boese, N. C. Handy, *Phys. Chem. Chem. Phys.* **1999**, *1*, 3939.
[17] S. Simon, J. Bertran, M. Soudpe, *J. Phys. Chem. A* **2001**, *105*, 4359.
[18] K. Balci, S. Akyuz, *J. Mol. Struct.* **2005**, *744*, 909.
[19] S. Melandri, M. E. Sanz, W. Caminati, P. G. Favero, Z. Kisiel, *J. Am. Chem. Soc.* **1998**, *120*, 11504.
[20] S. Akyuz, T. Akyuz, *J. Mol. Struct.* **2005**, *744*, 277.
[21] M. A. Munoz, P. Guardado, M. Galan, C. Carmona, M. Balon, *Biophys. Chem.* **2000**, *83*, 101.
[22] L. C. Zheng, S. R. Riemers, *J. Phys. Chem. A* **2005**, *109*, 1576.
[23] R. R. Shagidullin, A. Chemova, Z. G. Bazharova, H. Lii-Jenn, V. E. Kataev, S. A. Katsyuba, V. S. Reznik, *J. Mol. Struct.* **2004**, *707*, 1.
[24] S. Schlücker, J. Koster, R. K. Singh, B. P. Asthana, *J. Phys. Chem. A* **2007**, *111*, 5185.
[25] B. P. Asthana, H. Takahashi, W. Kiefer, *Chem. Phys. Lett.* **1983**, *94*, 41.
[26] M. Kreyenschmidt, H. H. Eysel, B. P. Asthana, *J. Raman Spectrosc.* **1993**, *24*, 645.
[27] H. Takahashi, K. Mamola, E. K. Player, *J. Mol. Spectrosc.* **1966**, *21*, 217.
[28] S. Schlücker, R. K. Singh, B. P. Asthana, J. Popp, W. Kiefer, *J. Phys. Chem. A* **2001**, *105*, 9983.

[29] V. Deckert, B. P. Asthana, P. C. Mishra, W. Kiefer, *J. Raman Spectrosc.* **1996**, *27*, 907.
[30] P. Raghuvansh (nee Briguvansh), S. K. Srivastava, R. K. Singh, B. P. Asthana, W. Kiefer, *Phys. Chem. Chem. Phys.* **2004**, *6*, 531.
[31] S. Schlücker, M. Heid, R. K. Singh, B. P. Asthana, J. Popp, W. Kiefer, *Z. Phys. Chem.* **2002**, *216*, 217.
[32] E. R. Berg, S. A. Freeman, D. D. Green, D. J. Ulness, *J. Phys. Chem. A* **2006**, *110*, 13434.
[33] A. D. Becke, *J. Chem. Phys.* **1992**, *97*, 9173 and **1993**, *98*, 5648.
[34] C. Lee, W. R. Yang, G. Parr, *Phys. Rev. B* **1988**, *37*, 785.
[35] M. J. Frisch, G. W. Trucks, H. B. Schlegel, G. E. Scuseria, M. A. Robb, J. R. Cheeseman, V. G. Zakrzewski, J. A. Montgomery Jr, R. E. Stratmann, J. C. Burant, S. Dapprich, J. M. Millam, A. D. Daniels, K. N. Kudin, M. C. Strain, O. Farkas, J. Tomasi, V. Barone, M. Cossi, R. Cammi, B. Mennucci, C. Pomelli, C. Adamo, S. Clifford, J. Ochterski, G. A. Petersson, P. Y. Ayala, Q. Cui, K. Morokuma, D. K. Malick, A. D. Rabuck, K. Raghavachari, J. B. Foresman, J. Cioslowski, J. V. Ortiz, A. G. Baboul, B. B. Stefanov, G. Liu, A. Liashenko, P. Piskorz, I. Komaromi, R. Gomperts, R. L. Martin, D. J. Fox, T. Keith, M. A. Al-Laham, C. Y. Peng, A. Nanayakkara, M. Challacombe, P. M. W. Gill, B. Johnson, W. Chen, M. W. Wong, J. L. Andres, C. Gonzalez, M. Head-Gordon, E. S. Replogle, J. A. Pople, *Gaussian 03*, Gaussian, Inc.: Pittsburgh, PA, **2003**.
[36] R. Dennington II, T. Keith, J. Millam, K. Eppinnett, W. L. Hovell, R. Gilliland, *GaussView 03*, R. Gilliland, Semichem, Inc.: Shawnee Mission, KS, **2003**.
[37] B. Mennuci, J. Tomasi, *J. Chem. Phys.* **1997**, *106*, 5151.
[38] E. F. Fileti, K. Coutinho, T. Malaspina, S. Canuto, *Phys. Rev. E* **2003**, *67*, 061504.
[39] R. K. Murray, D. K. Granner, P. A. Mayers, V. W. Rodwell, *Harper's Biochemistry*, Connecticut, 27th Ed.: **2006**.
[40] A. F. Bondarev, A. I. Mardaeva, *Opt. Spectrosc.* **1973**, *35*, 167.
[41] P. A. Egelstaff, *An Introduction to Liquid State*, Academic Press: New York, **1967**, p 10.
[42] Animesh K. Ojha, Sunil K. Srivastava, Ranjan K. Singh, B. P. Asthana, *J. Phys. Chem. A* **2006**, *110*, 9849.